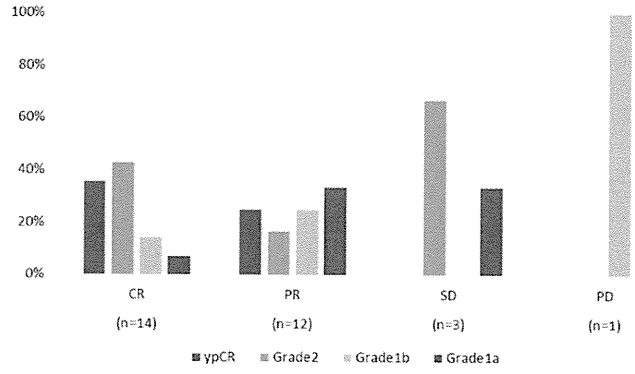

Figure 1. Discrepancies between clinical and histological objective responses. CR, complete response; PR, partial response; SD, stable disease; PD, progressive disease; ypCR, pathological complete response.

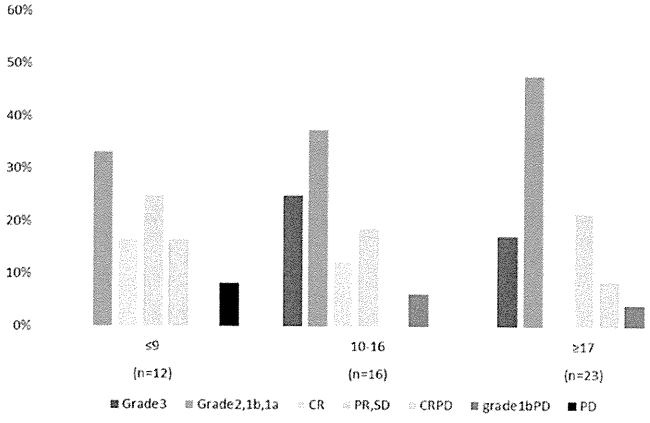

Figure 2. Results of the correlation between the objective response and the Hidaka RF output classification (HROC). CR, complete response; PR, partial response; SD, stable disease; CRPD, local CR but distant PD; PD, progressive disease. Grade: pathological complete response (pCR), grade 1bPD: local grade 1b but PD.

Tumors using MRI and PET/CT (16). Each resected specimen was examined for histological changes based on the histological criteria of the Japanese Classification of Colorectal Carcinoma. The CRPD group included patients in whom local tumors showed a complete response (CR), although new distant metastasis appeared. For the response assessment 8 weeks after HCRT, we evaluated CR as disappearance of the tumor on PET/CT and MRI and a positive to negative change in PET/CT. Adverse effects of these treatments were evaluated based on the criteria defined by the Common Terminology Criteria for Adverse Events (17).

Statistical analysis. SPSS Statistics (IBM, Armonk, NY, USA) version 21 was used to analyze all data. Mean values were compared using the Student's t-test. All reported p-values are two-tailed and were considered significant at $P<0.05$.

Results

Table I shows the patient characteristics. One patient had grade 3 perianal dermatitis. Only 2 patients with grade 2 disease wanted to decrease the dose of capecitabine (complete treatment, 96.1%). No output limiting symptoms were observed in 63.5% of the patients, whereas 30.2% suffered pain, and 2.0% had subcutaneous induration.

Good local control (ypCR + CR + CRPD) was observed in 32.7% of the patients in this study. Pathological complete response (ypCR) was observed in 15.7% of the total 51 patients and in 24.2% of the 33 patients who underwent surgery. Patients underwent surgery 8 weeks after HCRT. Abdominoperitoneal resection, lower anterior resection, intersphincteric resection, and partial resection were performed in 25, 43.7, 21.9, and 9.4% of the patients, respectively. One patient could

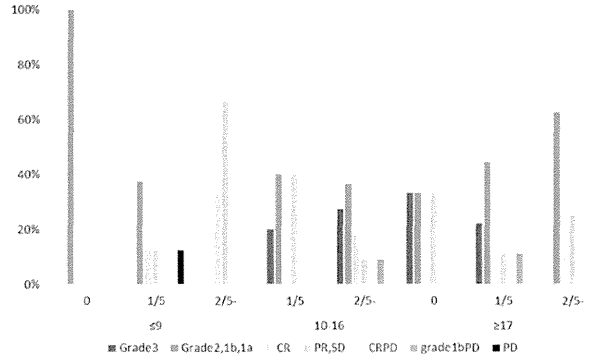

Figure 3. Results of the correlation among the objective response, the Hidaka RF output classification (HROC), and the incidence of output limiting symptoms. No output limiting symptoms, 1 output limiting symptoms, and ≥2 output limiting symptoms during the 5 thermal treatments are represented as 0, 1/5 and 2/5, respectively. CR, complete response; PR, partial response; SD, stable disease; CRPD, local CR but distant PD; PD, progressive disease. Grade; pathological complete response (pCR), grade 1bPD; local grade 1b but PD.

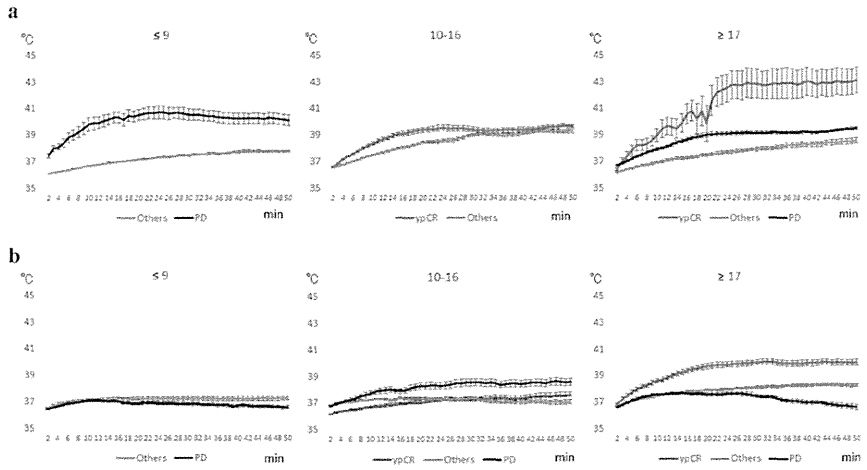

		Rectum	Time (min)	Skin	Time (min)
HROC	≤9	Others vs. PD	0-50	Others vs. PD	48-50
	10-16	ypCR vs. others	1-29	PD vs. ypCR	0-50
				PD vs. others	0-50
				ypCR vs. others	1-17
	≥17	ypCR vs. PD	0-50	ypCR vs. PD	0-50
		ypCR vs. others	0-50	ypCR vs. others	0-50
		Others vs. PD	0-50	Others vs. PD	31-50

Figure 4. Changes in rectal and skin temperatures during RF thermal treatment. (a) Rectal temperatures and (b) skin temperatures. Others: minor response [grade 2 + 1b + 1a + complete response (CR) + partial response (PR) + stable disease (SD)]. The results are presented as means ± standard errors. Significant differences were achieved (see table above) ($P<0.05$). PD, progressive disease; ypCR, pathological complete response.

not undergo resection of the primary tumor, and 5 patients could not undergo surgery due to progressive disease (PD); 13 (3 CR and 10 PR, SD) patients refused surgery mainly due to a permanent colostomy. Complete pathological response

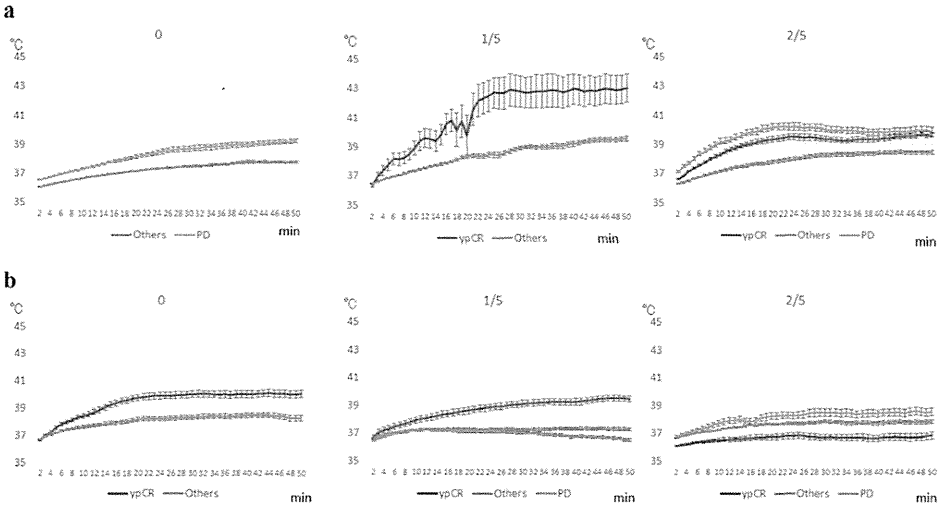

		Rectum	Time (min)	Skin	Time (min)
Incidence of output limiting symptoms	0	PD vs. others	0-5	ypCR vs. others	0-50
	1/5	ypCR vs. others	0-50	ypCR vs. others	0-50
				ypCR vs. PD	0-50
				Others vs. PD	36-50
	2/5	PD vs. ypCR	1-34	PD vs. ypCR	0-50
		PD vs . others	0-50	PD vs. others	-
		ypCR vs. others	0-50	PD vs. others	8-15

Figure 5. Changes in rectal and skin temperatures during irradiation (50 min) based on the incidence of output limiting symptoms and the objective response. (a) Rectal temperatures and (b) skin temperatures. The results are presented as means ± standard errors. Significant differences were achieved (see table above) ($P<0.05$). PD, progressive disease; ypCR, pathological complete response.

(ypCR), grade 2, grade 1b, and grade 1a were observed in 25.0, 31.3, 21.9, and 18.8% of 32 patients, whose tumors were resected, respectively. Two patients with grade 1b showed PD. A change from T2 to T0 was observed in 66.7%, T3 to T2 and T0 in 69.4%, T4 to T2 and T3 in 50.0%, N(+) to yN(-) in 66.7%, and M0 to M1 in 8.7% of the patients.

Fig. 1 illustrates the discrepancies between clinical and histological responses; CR and partial response (PR) were observed in 35.7 and 25.0% of patients showing ypCR, respectively, whereas no ypCR was observed in patients with both stable disease (SD) and PD.

Fig. 2 illustrates the results of the correlation between objective response and the HROC. Eight patients with ypCR presented with ≥10 points, whereas 4 patients with PD also presented with ≥10 points. There was no patients with ypCR among those with ≤9 points in the HROC.

Fig. 3 shows the results of the correlation between objective response, the HROC, and the incidence of output limiting symptoms. Patients with ypCR either experienced output limiting symptoms or were free of output limiting symptoms. PD was not observed in patients with ≥17 points without output limiting symptoms, whereas ypCR was not observed in patients with ≤9 points. Three patients with PD (CRPD+grade 1bPD) and output limiting symptoms presented with ≥17 points.

Fig. 4 illustrates the changes in rectal (Fig. 4a) and skin (Fig. 4b) temperatures during RF thermal treatment for 50 min, based on the HROC and objective response. For ≤9 points, the rectal temperature of PD patients was increased significantly when compared with the rectal temperature of the others, while, skin temperature of the others was slightly increased. For 10-16 points, the rectal temperature of the ypCR patients was significantly increased when compared with the rectal temperature of the others, while, skin temperatures of the PD patients was significantly increased when compared with skin temperatures of patients with pyCR and others ($P<0.05$). In regards to ≥17 points, rectal and skin temperatures of the ypCR patients were significantly increased when compared with these temperatures of others and PD ($P<0.05$).

Fig. 5 shows the changes in rectal (Fig. 5a) and skin (Fig. 5b) temperatures during RF treatment for 50 min, based on the incidence of output limiting symptoms and objective response. In patients without output limiting symptoms, rectal temperature

of the PD patients was significantly increased than those of others, while skin temperature of the ypCR patients was significantly increased when compared with the skin temperature of the others (P<0.05). In patients who suffered output limiting symptoms once during the 5 treatments, both rectal and skin temperatures of the ypCR patients were significantly increased when compared with those of the other responses (P<0.05). However, in patients who experienced output limiting symptoms ≥2 times, both rectal and skin temperatures of the PD patients showed significantly higher temperature increases than those with others and ypCR (P<0.05).

Based on the results of Figs. 4 and 5, two types of patients were identified: patients with or without increased temperatures, and consequently, those who benefited or those who did not; and patients with or without increased temperatures in both the ypCR and PD groups, even though they received similar RF outputs.

Discussion

In this retrospective and prospective study, we aimed to establish a standardized protocol for RF hyperthermia safety, and 15.7, 7.8, and 7.8% of patients experienced ypCR, CR, and CRPD, respectively; 31.4 and 13.7% of patients showed good local control (ypCR + CR + CRPD) and PD (CRPD + grade 1b PD + PD), respectively. All ypCR cases had ≥10 points, while no ypCR patients presented with ≤9 points according to the HROC. We also demonstrated that there were two types of patients: patients with or without increased temperatures and who consequently received a benefit or not from treatment, even though they received similar RF outputs. Previously, we had reported that all patients with clinical CR showed significantly higher increases in temperatures than those with other responses, whereas in PR + SD patients the increase of temperature or not depended on whether the patients experienced any output limiting symptoms or not, and consequently, had good or poor outcomes (15). Our results indicate that increased temperatures correlate with the clinical response but not the histological response; increased temperatures served to control tumors but not kill tumor cells.

Randomized NART for rectal cancer showed a ypCR rate ranging from 13 to 20%, with grade 3 toxicity ranging from 6 to 25% (18). Oxaliplatin-based neoadjuvant chemotherapy resulted in an increase in ypCR rates and grade 3 toxicity (19-21). For rectal cancers, NART plus capecitabine showed a ypCR rate ranging from 6.7 to 31%, with grade 3 toxicity ranging from 5 to 15% (22). Capecitabine plus IRMT showed a ypCR ranging from 14.1 to 30.6%, with grade 3 toxicity ranging from 11.1 to x17.6% (23). Lu *et al* reported a ypCR rate of 20%, grade 3 toxicity of 22%, and PD rates of 17% (24). Whereas NACR showed superior local tumor control and higher rates of side effects than our results, most studies failed to report PD cases.

The correlation between the efficacy of hyperthermia and temperature has been reported (25). Based on our results and other reports of NART, the following two questions were raised: i) no ypCR was observed among patients with ≤9 points, and ii) ypCR patients did not have increased temperature, but had a good outcome. These questions may be pivotal in predicting the response to hyperthermia based on the control mechanism of a set point of core temperatures and thermoregulation in individual patients.

In this study, we analyzed skin temperature as a simple reproducible marker. Thermal control of skin temperature depended on a fundamental homeostatic function. Therefore, skin thermoregulation depends on the thermoregulatory center and thermoreceptors on the skin (26). Recently an association was observed between thermoregulation and the transient receptor potential (TRP) family; TRP vaniloid-1 was one of the important factors for thermoregulation and was activated at a noxious heat range (>43˚C) or at temperatures above 32˚C, and it was correlated with pain threshold (27-29). The correlation between the TRP family and thermal treatment will be considered in the future.

In conclusion, we proposed a standardization of RF thermal treatment safety. Neothermia with chemoradiation is a potential new treatment for rectal cancer; further studies on preventing output limiting symptoms and evaluating thermoregulatory control mechanisms in individual patients are needed in the future.

Acknowledgements

We would like to thank all participating patients and the radiological technicians Mr S. Suda, Mr K. Sugawara, and Mr K. Jinbo for their assistance.

References

1. Roussakow S: The History of Hyperthermia Rise and Decline. Conference Papers in Medicine vol. 2013, article ID 428027, 2013. doi:10.1155/2013/428027.
2. Lee CK, Song CW, Rhee JG, Foy JA and Levitt SH: Clinical experience using 8 MHz radiofrequency capacitive hyperthermia in combination with radiotherapy: Results of a phase I/II study. Int J Radiat Oncol Biol Phys 32: 733-745, 1995.
3. Wiersma J, van Wieringen N, Crezee H and van Dijk JD: Delineation of potential hot spots for hyperthermia treatment planning optimisation. Int J Hyperthermia 23: 287-301, 2007.
4. Vasanthan A, Mitsumori M, Park JH, Zhi-Fan Z, Yu-Bin Z, Oliynychenko P, Tatsuzaki H, Tanaka Y and Hiraoka M: Regional hyperthermia combined with radiotherapy for uterine cervical cancers: A multi-institutional prospective randomized trial of the international atomic energy agency. Int J Radiat Oncol Biol Phys 61: 145-153, 2005.
5. Roussakow S: Critical analysis of randomized trials on hyperthermia: dubious effect and multiple biases. Conference Papers in Medicine vol. 2013, article ID 412186, 2013. doi:10.1155/2013/412186 2013.
6. van der Zee J, González González D, van Rhoon GC, van Dijk JD, van Putten WL and Hart AA; Dutch Deep Hyperthermia Group: Comparison of radiotherapy alone with radiotherapy plus hyperthermia in locally advanced pelvic tumours: A prospective, randomised, multicentre trial. Lancet 355: 1119-1125, 2000.
7. Gérard A, Buyse M, Nordlinger B, Loygue J, Pène F, Kempf P, Bosset JF, Gignoux M, Arnaud JP, Desaive C, *et al*: Preoperative radiotherapy as adjuvant treatment in rectal cancer. Final results of a randomized study of the European Organization for Research and Treatment of Cancer (EORTC). Ann Surg 208: 606-614, 1988.
8. Påhlman L and Glimelius B: Pre- or postoperative radiotherapy in rectal and rectosigmoid carcinoma. Report from a randomized multicenter trial. Ann Surg 211: 187-195, 1990.
9. No authors listed: Preoperative short-term radiation therapy in operable rectal carcinoma. A prospective randomized trial. Stockholm Rectal Cancer Study Group. Cancer 66: 49-55, 1990.
10. Bosset JF, Collette L, Calais G, Mineur L, Maingon P, Radosevic-Jelic L, Daban A, Bardet E, Beny A and Ollier JC; EORTC Radiotherapy Group Trial 22921: Chemotherapy with preoperative radiotherapy in rectal cancer. N Engl J Med 355: 1114-1123, 2006.

11. Gérard JP, Conroy T, Bonnetain F, Bouché O, Chapet O, Closon-Dejardin MT, Untereiner M, Leduc B, Francois E, Maurel J, *et al*: Preoperative radiotherapy with or without concurrent fluorouracil and leucovorin in T3-4 rectal cancers: Results of FFCD 9203. J Clin Oncol 24: 4620-4625, 2006.
12. Bosset JF, Calais G, Mineur L, Maingon P, Stojanovic-Rundic S, Bensadoun RJ, Bardet E, Beny A, Ollier JC, Bolla M, *et al*; EORTC Radiation Oncology Group: Fluorouracil-based adjuvant chemotherapy after preoperative chemoradiotherapy in rectal cancer: Long-term results of the EORTC 22921 randomised study. Lancet Oncol 15: 184-190, 2014.
13. Asao T, Sakurai H, Harashima K, Yamaguchi S, Tsutsumi S, Nonaka T, Shioya M, Nakano T and Kuwano H: The synchronization of chemotherapy to circadian rhythms and irradiation in pre-operative chemoradiation therapy with hyperthermia for local advanced rectal cancer. Int J Hyperthermia 22: 399-406, 2006.
14. Japanese Colon Cancer Association: Japanese Classification of Colon Carcinoma. 8th edition. Kanehara, Tokyo, 2013.
15. Shoji H, Motegi M, Osawa K, Okonogi N, Okazaki A, Andou Y, Asao T, Kuwano H, Takahashi T and Ogoshi K: Does standardization of radiofrequency hyperthermia benefit patients with malignancies? Ann Cancer Res Ther 22: 28-35, 2014.
16. Therasse P, Arbuck SG, Eisenhauer EA, Wanders J, Kaplan RS, Rubinstein L, Verweij J, Van Glabbeke M, van Oosterom AT, Christian MC, *et al*: New guidelines to evaluate the response to treatment in solid tumors. European Organization for Research and Treatment of Cancer, National Cancer Institute of the United States, National Cancer Institute of Canada. J Natl Cancer Inst 92: 205-216, 2000.
17. Common Terminology Criteria for Adverse Events (CTCAE): U.S. National Cancer Institute, Cancer Therapy Evaluation Program. http://ctep.cancer.gov/protocolDevelopment/electronic_applications/ctc.htm. Accessed December 2, 2014.
18. Gerard JP, Rostom Y, Gal J, Benchimol D, Ortholan C, Aschele C and Levi JM: Can we increase the chance of sphincter saving surgery in rectal cancer with neoadjuvant treatments: Lessons from a systematic review of recent randomized trials. Crit Rev Oncol Hematol 81: 21-28, 2012.
19. Ricardi U, Racca P, Franco P, Munoz F, Fanchini L, Rondi N, Dongiovanni V, Gabriele P, Cassoni P, Ciuffreda L, *et al*: Prospective phase II trial of neoadjuvant chemo-radiotherapy with oxaliplatin and capecitabine in locally advanced rectal cancer (XELOXART). Med Oncol 30: 581, 2013.
20. Passoni P, Fiorino C, Slim N, Ronzoni M, Ricci V, Di Palo S, De Nardi P, Orsenigo E, Tamburini A, De Cobelli F, *et al*: Feasibility of an adaptive strategy in preoperative radiochemotherapy for rectal cancer with image-guided tomotherapy: Boosting the dose to the shrinking tumor. Int J Radiat Oncol Biol Phys 87: 67-72, 2013.
21. Landry JC, Feng Y, Cohen SJ, Staley CA III, Whittington R, Sigurdson ER, Nimeiri H, Verma U, Prabhu RS and Benson AB: Phase 2 study of preoperative radiation with concurrent capecitabine, oxaliplatin, and bevacizumab followed by surgery and postoperative 5-fluorouracil, leucovorin, oxaliplatin (FOLFOX), and bevacizumab in patients with locally advanced rectal cancer: ECOG 3204. Cancer 119: 1521-1527, 2013.
22. Huang MY, Chen CF, Huang CM, Tsai HL, Yeh YS, Ma CJ, Wu CH, Lu CY, Chai CY, Huang CJ, *et al*: Helical tomotherapy combined with capecitabine in the preoperative treatment of locally advanced rectal cancer. Biomed Res Int 2014: 352083, 2014.
23. Hernando-Requejo O, López M, Cubillo A, Rodriguez A, Ciervide R, Valero J, Sánchez E, Garcia-Aranda M, Rodriguez J, Potdevin G, *et al*: Complete pathological responses in locally advanced rectal cancer after preoperative IMRT and integrated-boost chemoradiation. Strahlenther Onkol 190: 515-520, 2014.
24. Lu JY, Xiao Y, Qiu HZ, Wu B, Lin GL, Xu L, Zhang GN and Hu K: Clinical outcome of neoadjuvant chemoradiation therapy with oxaliplatin and capecitabine or 5-fluorouracil for locally advanced rectal cancer. J Surg Oncol 108: 213-219, 2013.
25. Kapp DS and Cox RS: Thermal treatment parameters are most predictive of outcome in patients with single tumor nodules per treatment field in recurrent adenocarcinoma of the breast. Int J Radiat Oncol Biol Phys 33: 887-899, 1995.
26. Romanovsky AA: Thermoregulation: Some concepts have changed. Functional architecture of the thermoregulatory system. Am J Physiol Regul Integr Comp Physiol 292: R37-R46, 2007.
27. Caterina MJ, Schumacher MA, Tominaga M, Rosen TA, Levine JD and Julius D: The capsaicin receptor: A heat-activated ion channel in the pain pathway. Nature 389: 816-824, 1997.
28. Tominaga M, Caterina MJ, Malmberg AB, Rosen TA, Gilbert H, Skinner K, Raumann BE, Basbaum AI and Julius D: The cloned capsaicin receptor integrates multiple pain-producing stimuli. Neuron 21: 531-543, 1998.
29. Yao J, Liu B and Qin F: Kinetic and energetic analysis of thermally activated TRPV1 channels. Biophys J 99: 1743-1753, 2010.

Nuclear heat shock protein 110 expression is associated with poor prognosis and chemotherapy resistance in gastric cancer

Akiharu Kimura[1], Kyoichi Ogata[1], Bolag Altan[1], Takehiko Yokobori[1], Munenori Ide[2], Erito Mochiki[3], Yoshitaka Toyomasu[1], Norimichi Kogure[1], Toru Yanoma[1], Masaki Suzuki[1], Tuya Bai[1], Tetsunari Oyama[2], Hiroyuki Kuwano[1]

[1]Department of General Surgical Science, Gunma University Graduate School of Medicine, Maebashi, Gunma, Japan

[2]Department of Diagnostic Pathology, Gunma University Graduate School of Medicine, Maebashi, Gunma, Japan

[3]Department of Digestive Tract and General Surgery, Saitama Medical Center, Saitama Medical University, Kawagoe, Saitama, Japan

Correspondence to: Hiroyuki Kuwano, **e-mail:** hkuwano@gunma-u.ac.jp

Keywords: *cancer progression, drug resistance, gastric cancer, heat shock protein, heat shock protein 110*

Received: *September 25, 2015* ***Accepted:*** *January 23, 2016* ***Published:*** *March 01, 2016*

ABSTRACT

Heat shock protein (HSP) expression is induced by the exposure to stress, such as fever, oxidative stress, chemical exposure, and irradiation. In cancer, HSP promotes the survival of malignant cells by inhibiting the induction of apoptosis. In colorectal cancer, a loss-of-function mutation of HSP110 (HSP110ΔE9) has been identified. HSP110ΔE9 inhibits the nuclear translocation of wild-type HSP110, which is important for its chaperone activity and anti-apoptotic effects. The patients carrying HSP110ΔE9 mutation exhibit high sensitivity to anticancer agents, such as oxaliplatin and 5-fluorouracil.There is still insufficient information about HSP110 localization, the clinicopathological significance of HSP110 expression, and its association with chemotherapy resistance in gastric cancer. Here, we found that high nuclear expression of HSP110 in gastric cancer tissues is associated with cancer progression, poor prognosis, and recurrence after adjuvant chemotherapy. *In vitro* results showed that HSP110 suppression increases the sensitivity to 5-fluorouracil and cisplatin of human gastric cancer cell lines. Our results suggest that nuclear HSP110 may be a new drug sensitivity marker for gastric cancer and a potential molecular therapeutic target for the treatment of gastric cancer patients with acquired anticancer drug resistance.

INTRODUCTION

Gastric cancer is one of the most common cancers worldwide and it is particularly prevalent in Asia [1]. Patients with early-stage gastric cancer have a good prognosis following endoscopic or surgical treatment [2], but advanced or recurrent gastric cancer patients have high mortality rates, due to chemotherapy resistance [3]. Therefore, the investigations of the mechanisms of chemotherapy resistance are necessary, in order to improve patient outcomes.

Heat shock proteins (HSPs) are molecular chaperones that facilitate the proper folding and function of proteins. The expression of HSPs is induced by the exposure to stress, such as fever, oxidative stress, chemical exposure, and irradiation [4, 5]. HSPs provide protection against protein aggregation, facilitate folding of nascent polypeptides, participate in the refolding of proteins that have been damaged, and sequester damaged proteins and target them for degradation [6, 7]. Mammalian HSPs are classified into several protein families based on their molecular weight, namely HSP25/HSP27, HSP40, HSP60, HSP70, HSP90, and HSP110 (also called HSP105) families [8, 9]. HSP70 family proteins are expressed in the cytoplasm and nucleus of mammalian cells [10]. HSP105α and HSP105β, the alternatively spliced products of *HSP110* family, are expressed in the cytoplasm (HSP105α) and in nucleus (HSP105β) [11]. Previously, it was reported that nuclear HSPs behave as molecular chaperones in cells [10].

HSPs were shown to be overexpressed in a wide range of human carcinomas, including both solid tumors and hematological malignancies [7, 12, 13]. In cancer, HSP promotes the survival of malignant cells by

protecting several oncoproteins from degradation and inhibiting the induction of apoptosis. This suggests that HSP roles are beneficial for cancerous cells and therefore deleterious for cancer patients [14]. High levels of HSPs may correlate with poor prognosis in several types of cancer. For example, high levels of HSP27 were shown to correlate with poor prognosis in ovarian cancer [15], and HSP60 overexpression was correlated with tumor progression and poor prognosis in colon cancer [16] and prostate carcinoma [17]. The elevated expression of HSP70 is associated with poor prognosis in breast [18] and endometrial [19] cancers, while high HSP90 expression is associated with poor prognosis in invasive ductal breast carcinoma [20] but with good prognosis in endometrial cancer [19]. Furthermore, it was reported that various HSPs, including HSP70 and HSP90, are associated with increased chemosensitivity and may represent potential therapeutic targets in refractory malignancies [21–23].

Antitumor response generated by autologous tumor-derived HSP/GRPs (*e.g.*, Hsp70, Hsp90, Grp94/gp96, and calreticulin) has been well documented [9, 24, 25]. Studies over the last decade showed that certain tumor-derived HSPs can serve as effective cancer vaccines, and this has been attributed to an HSP-carried peptide antigenic 'fingerprint' of the tumor [24, 26–29].

Dorard *et al.* identified a loss-of-function mutation of HSP110 (HSP110ΔE9) in colorectal cancers with microsatellite instability [30]. HSP110ΔE9 lacks a substrate-binding domain, and it is unable to play a role of a molecular chaperone for other HSPs (HSP70 or HSP27). Mutant HSP110ΔE9 protein associates with wild-type HSP110, blocking its translocation into the nucleus and its chaperone functions. Therefore, HSP110ΔE9 overexpression enhances the sensitivity of tumors to anticancer agents, such as oxaliplatin and 5-fluorouracil (5-FU) [30].

However, HSP110 localization, its clinicopathological significance, and its association with chemotherapy resistance in gastric cancer have not been completely elucidated. The objectives of this study were to clarify the significance of HSP110 expression in gastric cancer patients and to assess the effects of HSP110 suppression on chemosensitivity.

RESULTS

Clinical significance of nuclear HSP110 expression in gastric cancer patients

Nuclear HSP110 expression was immunohistochemically evaluated using a tissue microarray that included 210 gastric cancer samples. HSP110 expression in cancer tissues was higher compared with non-cancerous tissues. In the cancer tissues, nucleus and cytoplasm were positive for HSP110 immunostaining (Figure 1A and 1B). In non-cancerous tissues, no or weak staining was observed for HSP110. Nuclear HSP110 expression scores in 210 gastric cancer samples were as follows: 0, 17 (8.1%) samples; 1+, 72 (34.3%) samples; 2+, 80 (38.1%) samples; and 3+, 41(19.5%) samples. Eighty-nine (42.4%) samples were included in the low expression group, and 121 (57.6%) samples were included in the high expression group. The relationship of nuclear HSP110 expression and clinicopathological factors from 210 gastric cancer patients is presented in Table 1. High nuclear expression of HSP110 was significantly associated with venous invasion (P = 0.0464). The overall survival rate in the high expression group was significantly lower compared with the low expression group (P = 0.0169; Figure 2). Multivariate regression analysis revealed that high expression of nuclear

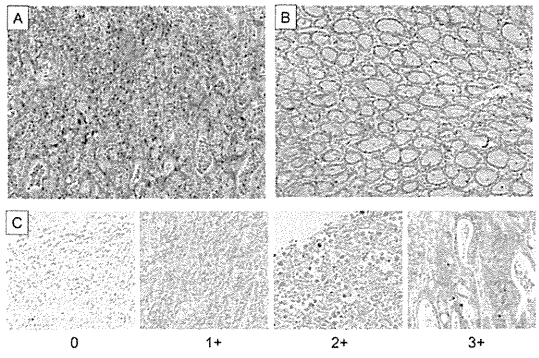

Figure 1: Immunohistochemical staining of HSP110 in primary gastric cancer samples. (**A**) Cancerous tissue; (**B**) Non-cancerous tissue (original magnification, × 200). (**C**) Tissue microarray samples (original magnification, 200 ×). The intensity of nuclear HSP110 staining was scored as follows: 0, no staining; 1+, weak staining; 2+, moderate staining; 3+, strong staining.

Table 1: The relationship between clinicopathological characteristics of gastric cancer patients and the nuclear HSP110 expression levels

Factors	HSP110 expression in gastric cancer (n = 210)		
	Low (n = 89)	High (n = 121)	P value
Age (mean ± standard error)	63.1 ± 1.2	65.7 ± 1.0	0.1007
Gender, n (%)			
Male	66 (44.9%)	81 (55.1%)	0.2574
Female	23 (36.5%)	40 (63.5%)	
Histology, n (%)			
Well, Moderate	33 (41.8%)	46 (58.2%)	0.8897
Poor, Signet	56 (42.7%)	75 (57.3%)	
Depth, n (%)			
sm, mp, ss	48 (40.7%)	70 (59.3%)	0.8266
se, si	41 (44.6%)	51 (55.4%)	
Lymph node metastasis, n (%)			
Absent	30 (44.8%)	37 (55.2%)	0.6311
Present	59 (41.3%)	84 (58.7%)	
Lymphatic invasion, n (%)			
Absent	9 (47.4%)	10 (52.6%)	0.6459
Present	80 (41.9%)	111 (58.1%)	
Venous invasion, n (%)			
Absent	71 (46.7%)	81 (53.3%)	0.0464*
Present	18 (31.6%)	39 (68.4%)	
Stage, n (%)			
I	12 (36.4%)	21 (63.6%)	0.5754
II	33 (47.8%)	36 (52.2%)	
III	35 (42.7%)	47 (57.3%)	
IV	9 (34.6%)	17 (65.4%)	

*$P < 0.05$.

Well: well differentiated, Moderate: moderately differentiated, Poor: poorly differentiated, Signet: signet ring cells, sm: submucosa, mp: muscularis propria, ss: subserosa, se: serosa exposed, si: serosa infiltrating.

HSP110 is an independent prognostic factor for gastric cancer outcome (P = 0.0068), as are the tumor depth (P < 0.001) and venous invasion (P = 0.0276; Table 2). Additionally, we assessed cytoplasmic HSP110 expression in 210 gastric cancer tissue samples. No significant difference in prognosis was observed between the cytoplasmic HSP110 high expression group and low expression group (P = 0.6884, Supplementary Figure S1). Furthermore, additional analysis was performed in order to evaluate the significance of total HSP110 expression in gastric cancer tissues. The high cytoplasmic and nuclear HSP110 expression groups were defined as total HSP110 high expression group (n = 74). The low cytoplasmic and nuclear HSP110 expression groups were defined as total HSP110 low expression group (n = 73). There was no significant prognostic difference between the total HSP110 high expression group and low expression group (P = 0.2021, Supplementary Figure S2). The relationship between total HSP110 expression and clinicopathological factors is shown in Supplementary Table S1. No significant relationships were found between total HSP110 expression and clinicopathological factors, with the only exception being patients' ages.

Prognostic significance of nuclear HSP110 expression in gastric cancer patients who received adjuvant chemotherapy

Forty-eight of the 210 gastric cancer patients received 5-FU-based adjuvant chemotherapy. We evaluated the correlation between nuclear HSP110 expression and prognosis in these patients (Figure 3A and 3B). Among patients who received adjuvant chemotherapy, the overall survival rate in the high expression group was significantly lower compared with the low expression group ($P = 0.0364$). There was no significant difference in disease-free survival between the two groups, but the disease-free survival rate in the high expression group tended to be lower compared with the low expression group ($P = 0.0743$).

HSP110 expression in gastric cancer cell lines

HSP110 expression was detected using western blot in all human gastric cancer cell lines (MKN7, MKN45, MKN74, AZ521) (Figure 4A). MKN7 and MKN45 were further used for the *in vitro* analyses of the effects of HSP110 suppression in gastric cancer cell lines. HSP110 expression was suppressed in MKN7 and MKN45 cells treated with HSP110 siRNA (Figure 4B and 4C).

The effects of HSP110 suppression on the chemosensitivity of gastric cancer cell lines

We evaluated the correlation between HSP110 suppression and the chemosensitivity of gastric cancer cell lines. Following HSP110 knockdown, MKN7 and MKN45 cells were treated with 5-FU or cisplatin. The sensitivity to 5-FU and cisplatin of HSP110 siRNA-treated cells was significantly higher compared with the parent and control cells ($P < 0.05$; Figure 4D).

DISCUSSION

Here, we determined that high nuclear expression of HSP110 in gastric cancer tissues is associated with cancer progression and poor prognosis. Among patients who received adjuvant chemotherapy, those included in the high HSP110 expression group showed significantly shorter overall survival compared with the low expression group. *In vitro* study showed that HSP110 suppression increases the sensitivity to 5-FU and cisplatin in human gastric cancer cell lines.

Immunohistochemical analysis demonstrated that the high expression of nuclear HSP110 is associated with poor overall survival. Based on the multivariate analysis of the factors affecting overall survival, the high expression of nuclear HSP110 was shown to be an independent prognostic factor. Previously, it was reported that the high expression of HSP110 is associated with poor prognosis in lung adenocarcinoma [31] and colorectal cancer [32], and our results are consistent with these reports. The chaperoning properties of HSP110 are integral to the ability of these molecules to modulate immune functions and for the development of large chaperone complex vaccines for cancer immunotherapy [9]. Nakajima *et al.* reported that high cytoplasmic HSP110 expression induces CD4+ T lymphocyte infiltration, which was shown to be associated with good prognosis in esophageal cancer [33]. We assessed total and cytoplasmic HSP110 expression

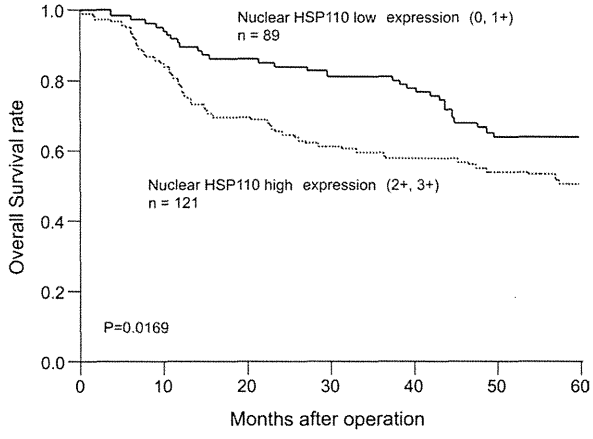

Figure 2: Overall survival of gastric cancer patients according to the nuclear HSP110 expression. The overall survival in the nuclear HSP110 high expression group was significantly shorter compared with the low expression group ($P = 0.0169$).

Table 2: Univariate and multivariate analyses of clinicopathological factors affecting overall survival rates after surgery

Clinicopathological variables	Univariate analysis			Multivariate analysis		
	RR	95% CI	*P* value	RR	95% CI	*P* value
Age (< 65 years/ ≥ 65 years)	1.11	0.90–1.37	0.3209	-	-	-
Gender (male/female)	0.9	0.71–1.13	0.3873	-	-	-
Histology (differentiated/undifferentiated)	1.11	0.89–1.38	0.3546	-	-	-
Depth (sm, mp, ss/se, si)	1.83	1.48–2.29	0.0000*	1.74	1.39–2.19	< 0.001*
Lymph node metastasis (absent/present)	1.59	1.24–2.11	0.0002*	1.31	0.99–1.78	0.0579
Lymphatic invasion (absent/present)	1.88	1.15–3.79	0.0081*	1.12	0.64–2.33	0.7230
Venous invasion (absent/present)	1.47	1.19–1.83	0.006*	1.29	1.03–1.60	0.0276*
HSP110 expression (low/high)	1.3	1.05–1.63	0.0155*	1.35	1.09–1.70	0.0068*

*$P < 0.05$.

RR: Relative risk, CI: Confidence interval, sm: submucosa, mp: muscularis propria, ss: subserosa, se: serosa exposed, si: serosa infiltrating.

in gastric cancer samples, but no significant prognostic differences were observed in the total and cytoplasmic HSP110 expression between the high and low groups (Supplementary Figures S1, S2). It was previously reported that wild-type nuclear, rather than cytoplasmic, HSP110 prevents the induction of apoptosis in colorectal cancer cells [30]. Therefore, we suggest that nuclear HSP110 expression levels may be a useful prognostic and drug sensitivity marker for gastric cancer.

In this study, the high expression of nuclear HSP110 was shown to be associated with venous invasion (Table 1). HSPs promote cancer progression in several cancer types, and Gong *et al.* [34] reported that the invasion potential of hepatocarcinoma cells is increased by HMGB1-induced tumor NF-κB signaling, through the activation of HSP70. Sims *et al.* [35] reported that extracellular HSP70 and HSP90α contribute to the matrix metalloproteinase-2 activation and breast cancer cell migration and invasion.

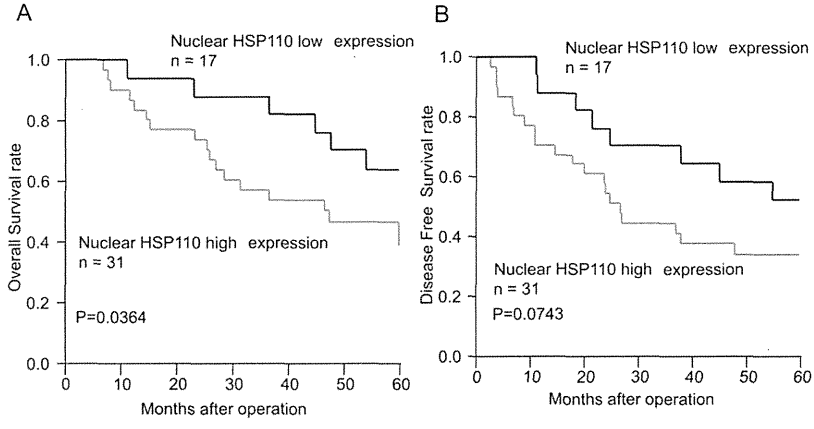

Figure 3: The survival curves of gastric cancer patients who received adjuvant chemotherapy according to nuclear HSP110 expression. (**A**) Overall survival. (**B**) Disease-free survival. Among the patients who received adjuvant chemotherapy, the overall survival rate in the nuclear HSP110 high expression group was significantly lower compared with the low expression group ($P = 0.0364$). No significant difference in disease-free survival was observed between these groups; however, the disease-free survival rate in the high expression group tended to be lower compared with the low expression group ($P = 0.0743$).

It has also been reported that HSP110 is co-expressed with HSP70 and HSP90 during stress, and that it promotes HSP90 activity and may function as a nucleotide exchange factor for cytosolic HSP70 [36]. We elucidated whether HSP110 expression can facilitate cancer invasion through the activation of HSP70 and HSP90.

Hosaka *et al.* [37] reported that HSP110 suppression induces apoptosis in cancer cell lines but not in fibroblasts. Dorard *et al.* [30] identified a loss-of-function mutation of HSP110 (HSP110ΔE9) in colorectal cancer with microsatellite instability. HSP110ΔE9 overexpression enhanced cancer cell sensitivity to anticancer agents. Here, low nuclear HSP110 expression group had better prognosis compared with the high expression group, and HSP110 suppression was shown to increase cell sensitivity to 5-FU and cisplatin in human gastric cancer cell lines, which is consistent with the previous reports. Novel treatment strategies, combining an HSP110 inhibitor and an anticancer agent, may be effective for the treatment of gastric cancer patients with acquired anticancer drug resistance.

Previously, HSP110 was identified as a cancer antigen in various human carcinomas [31, 32]. We report here that the high expression of the nuclear HSP110 was observed in gastric cancer patients. Wang *et al.* [29] developed a vaccine composed of a recombinant protein coupled with large heat shock protein. Our results suggest that chemosensitivity may decrease due to heat stress-induced HSP110 expression. Therefore, various vaccines, which may utilize HSPs (*i.e.*, covalent coupling, isolation of HSPs with antigens attached, recombinant vaccines made by heat-denaturation of full-length antigens and HSP110) may be useful in anticancer treatments.

HSP110-specific siRNAs were used to suppress the expression of HSP110 in gastric cancer cell lines, which presents a limitation of this study. Therefore, total HSP110 expression was suppressed, and not only the specific nuclear HSP110 expression. Total HP110 expression was strongly suppressed in MKN7 and MKN45 by the HSP110-specific siRNA, but this is probably the consequence of the suppression of both nuclear and cytoplasmic HSP110 expression.

In conclusion, the high expression of nuclear HSP110 was shown to be associated with cancer progression, poor prognosis, and recurrence after adjuvant

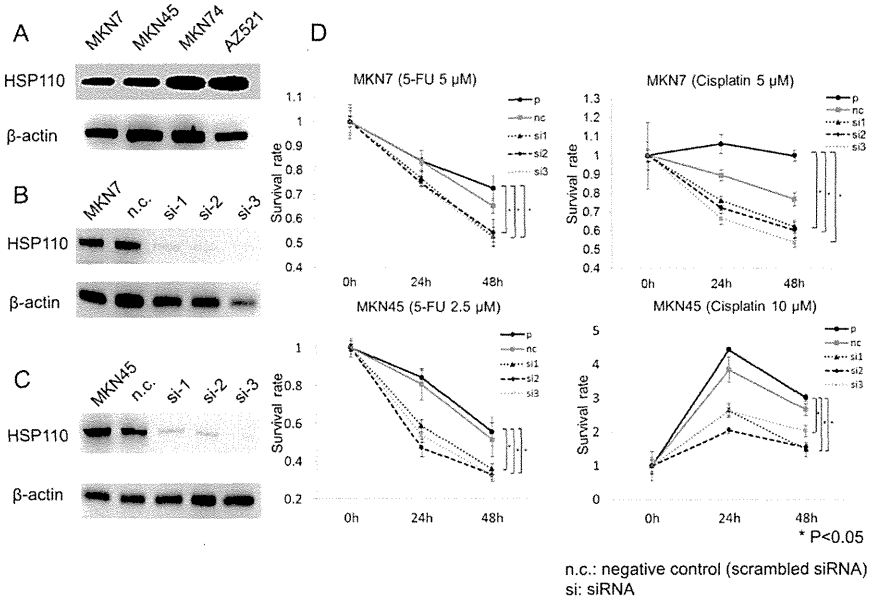

Figure 4: Functional analysis of human gastric cancer cell lines treated with HSP110 siRNA. (**A**) The expression of HSP110 in human gastric cancer cell lines was assessed by western blot. β-actin was used as the loading control. (**B**) HSP110 expression was suppressed using HSP110 siRNA (MKN7); (**C**) HSP110 suppression using HSP110 siRNA (MKN45). (**D**) The effects of HSP110 suppression on chemosensitivity of MKN7 and MKN45 cells. Both MKN7 and MKN45 cells showed a significantly increased sensitivity to 5-fluorouracil in HSP110 siRNA-treated groups, compared with the parent and control cells ($P < 0.05$). n.c.: negative control (scrambled siRNA), si: siRNA.

chemotherapy in gastric cancer patients. Furthermore, HSP110 suppression increased the sensitivity to 5-FU and cisplatin in the human gastric cancer cell lines. Our results suggest that nuclear HSP110 expression in gastric cancer may be a new prognostic and drug sensitivity marker, and HSP110 may serve as a new molecular therapeutic target for the treatment of refractory gastric cancer.

METHODS

Patients and samples

Primary gastric cancer tissues were obtained from gastric cancer patients (n = 210; 147 men and 63 women) who underwent radical gastrectomy at the Department of General Surgical Science, Gunma University Hospital, Japan, between January 1999 and May 2006. The stage of gastric cancer was described according to the classification of gastric carcinoma of the Japanese Gastric Cancer Association's 3rd English edition [38]. Forty-eight patients received 5-FU-based adjuvant chemotherapy between January 2003 and May 2006. The correlation between HSP110 expression and clinicopathological factors and prognosis was evaluated in these patients. Written informed consents were obtained from all patients according to institutional guidelines.

Tissue microarray analysis and immunohistochemical staining

Tumor samples were fixed in formalin, embedded in paraffin, and stored in the archives of the Clinical Department of Pathology, Gunma University Hospital, Japan. For 210 gastric cancer patients, one paraffin block containing representative non-necrotic tumor areas was selected, and gastric cancer tissue cores (2.0 mm diameter per tumor) were sampled from the representative areas and transferred into the paraffin block using a tissue arraying instrument (Beecher Instruments, Silver Spring, MD, USA). Cores were arranged into quad tissue array blocks, with each containing 50–55 tumor cores. Tissue microarray blocks were cut into 3.5-μm thick sections, and were used for the subsequent immunohistochemical staining. Additionally, 4-μm sections were cut from the paraffin blocks of 10 gastric cancer samples, selected among 210 gastric cancer patients for validation.

All sections were incubated at 60°C for 60 min and deparaffinized in xylene. Afterward, these sections were rehydrated and incubated with fresh 0.3% hydrogen peroxide in 100% methanol for 30 min at room temperature, in order to block endogenous peroxidase activity. Following the rehydration through a graded series of ethanol treatments, the sections were heated in boiling water and soaked in Immunosaver (Nishin EM, Tokyo, Japan) at 98°C for 90 min. Non-specific binding sites were blocked by incubating the sections with Protein Block Serum-Free (DAKO, Carpinteria, CA, USA) for 30 min. A rabbit monoclonal anti-HSP110 antibody (GeneTex, CA, USA) was applied at 1:100 dilution, for 24 h at 4°C. The primary antibody was visualized using the Histofine Simple Stain MAX-PO (MULTI) (Nichirei, Tokyo, Japan) according to the instruction manual. A chromogen, 3,3-diaminobenzidine tetrahydrochloride, was applied as a 0.02% solution containing 0.005% hydrogen peroxide in 50 mM ammonium acetate-citrate acid buffer (pH 6.0). The sections were lightly counterstained with Mayer's hematoxylin and mounted. The evaluation of immunohistochemical staining was performed by two independent researchers who were blinded to the patients' data. We focused on nuclear HSP110 expression, and the intensity of nuclear HSP110 staining was scored as follows: 0, no staining; 1+, weak staining; 2+, moderate staining; 3+, strong staining. Gastric cancer patients were assigned to the nuclear HSP110 low expression group (0, 1+) or high expression group (2+, 3+), according to staining score (Figure 1C). Additionally, the tissues adjacent to the cancerous tissues in the tissue microarray samples were considered non-cancerous tissue. We evaluated the expression of HSP110 in the non-cancerous tissue of these 10 samples, for validation. The non-cancerous tissue was defined as the normal gastric mucosa tissue or stromal cells.

Cell culture

The human gastric cancer cell lines MKN7, MKN45, MKN74, and AZ521 were used in this study. These cell lines were obtained from RIKEN BRC through the National Bio-Resource Project of MEXT, Tokyo, Japan. The cells were cultured in RPMI 1640 medium (Wako, Osaka, Japan) supplemented with 10% FBS and 1% penicillin-streptomycin (Invitrogen, Carlsbad, CA, USA).

siRNA transfection

HSP110-specific siRNA was purchased from Bonac Corporation (Fukuoka, Japan). MKN7 and MKN45 cells were plated at a density of 1.0×10^6 cells per well in 100 μl of Opti-MEM I Reduced Serum Medium (Invitrogen, Carlsbad, CA, USA). Twenty nM of HSP110-specific siRNA 1, 2, 3 and scrambled siRNA (negative control) were added to the cells, and cells were transfected with siRNAs using an electroporator (CUY-21 EDIT II; BEX, Tokyo, Japan), according to the manufacturer's instructions. Poring pulses were applied at 125 V (pulse length, 10.0 ms; 1 pulse; interval, 40.0 ms), and transfer pulses were applied at 10 V (pulse length, 50.0 ms; 5 pulses; interval, 50.0 ms). After 72 h of incubation, further experiments were performed.

Protein extraction and western blot analysis

Western blotting was performed to confirm the expression of HSP110 and β-actin in gastric cancer cell lines. Transfected cells were incubated for 72 h, and total proteins were extracted from MKN7, MKN45, MKN74, and AZ521 cells using PRO-PREP Protein Extraction Solution Kit (iNtRON Biotechnology, Sungnam, Kyungki-Do, Korea). The proteins were separated on 4–12% Bis-Tris Mini Gels (Life Technologies Corporation, Carlsbad, CA, USA), and transferred to membranes using an iBlot Dry Blotting System (Life Technologies Corporation, Carlsbad, CA, USA). The membranes were incubated overnight at 4°C with rabbit monoclonal anti-HSP110 antibody (1:1000; GeneTex, CA, USA) and anti-β-actin antibody (1:1000; Sigma-Aldrich, St Louis, MO, USA). Following this, the membranes were incubated with horseradish peroxidase-conjugated anti-rabbit secondary antibodies, and the target proteins were detected with the ECL Prime Western Blotting Detection System (GE Healthcare, Tokyo, Japan) using Image Quant LAS4000 (GE Healthcare Life Sciences, UK).

Chemosensitivity assay

Water-soluble tetrazolium-8 (Cell Counting Kit-8; Dojindo Laboratories, Japan) was used in order to evaluate the sensitivity to cisplatin and 5-FU. After 72 h of incubation following the transfection, MKN7 and MKN45 cells were seeded (1×10^4 cells/well) into 96-well plates in 100 μl of RPMI 1640 medium containing 20% FBS before drug exposure. After 24 h of pre-incubation, 10 μl of Cell Counting Kit-8 reagent were added, and the cells were additionally incubated for 2 h at 37°C. The absorbance of each well was detected at 450 nm using an xMark Microplate Absorbance Spectrophotometer (Bio Rad, Hercules, CA, USA). Afterward, the cells were treated with various concentrations of cisplatin and 5-FU for 48 h. Viability was determined using colorimetry by measuring absorbance every 24 h.

Statistical analysis

Data for continuous variables were expressed as mean ± standard error of the mean. Significance was determined using Student's *t*-test and analysis of variance. The statistical analysis of the immunohistochemical staining results was performed using the chi-squared test. Survival curves were generated according to the Kaplan-Meier method and analyzed using the log-rank test. Prognostic factors were examined by univariate and multivariate analyses using a Cox proportional hazards model. Results were considered statistically significant when P value was < 0.05. All statistical analyses were performed using JMP software, version 12 (SAS Institute Inc., Cary, NC, USA).

ACKNOWLEDGMENTS AND FUNDING

The authors thank Ms. Yukie Saito, Ms. Tomoko Yano, Ms. Tomoko Ubukata, Ms. Yuka Matsui, Ms. Ayaka Ishida, and Ayaka Ishikubo for their excellent assistance.

CONFLICTS OF INTEREST

None.

REFERENCES

1. Ferlay J, Shin HR, Bray F, Forman D, Mathers C, Parkin DM. Estimates of worldwide burden of cancer in 2008: GLOBOCAN 2008. Int J Cancer. 2010; 127:2893–2917.
2. Uedo N, Iishi H, Tatsuta M, Ishihara R, Higashino K, Takeuchi Y, Imanaka K, Yamada T, Yamamoto S, Tsukuma H, Ishiguro S. Longterm outcomes after endoscopic mucosal resection for early gastric cancer. Gastric Cancer. 2006; 9:88–92.
3. Cervantes A, Roselló S, Roda D, Rodriguez-Braun E. The treatment of advanced gastric cancer: current strategies and future perspectives. Ann Oncol. 2008; 19 Suppl 5: v103–107.
4. Lindquist S, Craig EA. The heat-shock proteins. Annu Rev Genet. 1988; 22:631–677.
5. Young JC, Agashe VR, Siegers K, Hartl FU. Pathways of chaperone-mediated protein folding in the cytosol. Nat Rev Mol Cell Biol. 2004; 5:781–791.
6. Hartl FU. Molecular chaperones in cellular protein folding. Nature. 1996; 381:571–579.
7. Soo ET, Yip GW, Lwin ZM, Kumar SD, Bay BH. Heat shock proteins as novel therapeutic targets in cancer. *in vivo*. 2008; 22:311–315.
8. Subjeck JR, Shyy TT. Stress protein systems of mammalian cells. Am J Physiol. 1986; 250:C1–17.
9. Wang XY, Subjeck JR. High molecular weight stress proteins: Identification, cloning and utilisation in cancer immunotherapy. Int J Hyperthermia. 2013; 29:364–375.
10. Welch WJ, Feramisco JR. Nuclear and nucleolar localization of the 72,000-dalton heat shock protein in heat-shocked mammalian cells. J Biol Chem. 1984; 259:4501–4513.
11. Saito Y, Yamagishi N, Hatayama T. Different localization of Hsp105 family proteins in mammalian cells. Exp Cell Res. 2007; 313:3707–3717.
12. Whitesell L, Lindquist SL. HSP90 and the chaperoning of cancer. Nat Rev Cancer. 2005; 5:761–772.
13. Chant ID, Rose PE, Morris AG. Analysis of heat-shock protein expression in myeloid leukaemia cells by flow cytometry. Br J Haematol. 1995; 90:163–168.
14. Rappa F, Farina F, Zummo G, David S, Campanella C, Carini F, Tomasello G, Damiani P, Cappello F, DE Macario EC, Macario AJ. HSP-molecular chaperones in cancer biogenesis

and tumor therapy: an overview. Anticancer Res. 2012; 32:5139–5150.

15. Langdon SP, Rabiasz GJ, Hirst GL, King RJ, Hawkins RA, Smyth JF, Miller WR. Expression of the heat shock protein HSP27 in human ovarian cancer. Clin Cancer Res. 1995; 1:1603–1609.
16. Cappello F, David S, Rappa F, Bucchieri F, Marasà L, Bartolotta TE, Farina F, Zummo G. The expression of HSP60 and HSP10 in large bowel carcinomas with lymph node metastase. BMC Cancer. 2005; 5:139.
17. Cappello F, Rappa F, David S, Anzalone R, Zummo G. Immunohistochemical evaluation of PCNA, p53, HSP60, HSP10 and MUC-2 presence and expression in prostate carcinogenesis. Anticancer Res. 2003; 23:1325–1331.
18. Lazaris ACh, Chatzigianni EB, Panoussopoulos D, Tzimas GN, Davaris PS, Golematis BCh. Proliferating cell nuclear antigen and heat shock protein 70 immunolocalization in invasive ductal breast cancer not otherwise specified. Breast Cancer Res Treat. 1997; 43:43–51.
19. Nanbu K, Konishi I, Komatsu T, Mandai M, Yamamoto S, Kuroda H, Koshiyama M, Mori T. Expression of heat shock proteins HSP70 and HSP90 in endometrial carcinomas. Correlation with clinicopathology, sex steroid receptor status, and p53 protein expression. Cancer. 1996; 77:330–338.
20. Pick E, Kluger Y, Giltnane JM, Moeder C, Camp RL, Rimm DL, Kluger HM. High HSP90 expression is associated with decreased survival in breast cancer. Cancer Res. 2007; 67:2932–2937.
21. He LF, Guan KP, Yan Z, Ye HY, Xu KX, Ren L, Hou SK. Enhanced sensitivity to mitomycin C by abating heat shock protein 70 expression in human bladder cancer cell line of BIU-87. Chin Med J (Engl). 2005; 118:1965–1972.
22. Lai CH, Park KS, Lee DH, Alberobello AT, Raffeld M, Pierobon M, Pin E, Petricoin Iii EF, Wang Y, Giaccone G. HSP-90 inhibitor ganetespib is synergistic with doxorubicin in small cell lung cancer. Oncogene. 2014; 33:4867–4876.
23. Fang X, Jiang Y, Feng L, Chen H, Zhen C, Ding M, Wang X. Blockade of PI3K/AKT pathway enhances sensitivity of Raji cells to chemotherapy through down-regulation of HSP70. Cancer Cell Int. 2013; 13:48.
24. Tamura Y, Peng P, Liu K, Daou M, Srivastava PK. Immunotherapy of tumors with autologous tumor-derived heat shock protein preparations. Science. 1997; 278: 117–120.
25. Vanaja DK, Grossmann ME, Celis E, Young CY. Tumor prevention and antitumor immunity with heat shock protein 70 induced by 15-deoxy-delta12, 14-prostaglandin J2 in transgenic adenocarcinoma of mouse prostate cells. Cancer Res. 2000; 60:4714–4718.
26. Graner M, Raymond A, Romney D, He L, Whitesell L, Katsanis E. Immunoprotective activities of multiple chaperone proteins isolated from murine B-cell leukemia/lymphoma. Clin Cancer Res. 2000; 6:909–915.
27. Wang XY, Kazim L, Repasky EA, Subjeck JR. Characterization of heat shock protein 110 and glucose-regulated protein 170 as cancer vaccines and the effect of fever-range hyperthermia on vaccine activity. J Immunol. 2001; 166:490–497.
28. Srivastava P. Interaction of heat shock proteins with peptides and antigen presenting cells: chaperoning of the innate and adaptive immune responses. Annu Rev Immunol. 2002; 20:395–425.
29. Wang XY, Yi H, Yu X, Zuo D, Subjeck JR. Enhancing antigen cross-presentation and T-cell priming by complexing protein antigen to recombinant large heat-shock protein. Methods Mol Biol. 2011; 787:277–287.
30. Dorard C, de Thonel A, Collura A, Marisa L, Svrcek M, Lagrange A, Jego G, Wanherdrick K, Joly AL, Buhard O, Gobbo J, Penard-Lacronique V, Zouali H, et al. Expression of a mutant HSP110 sensitizes colorectal cancer cells to chemotherapy and improves disease prognosis. Nat Med. 2011; 17:1283–1289.
31. Oda T, Morii E, Inoue M, Ikeda J, Aozasa K, Okumura M. Prognostic significance of heat shock protein 105 in lung adenocarcinoma. Mol Med Rep. 2009; 2:603–607.
32. Slaby O, Sobkova K, Svoboda M, Garajova I, Fabian P, Hrstka R, Nenutil R, Sachlova M, Kocakova I, Michalek J, Smerdova T, Knoflickova D, Vyzula R. Significant overexpression of Hsp110 gene during colorectal cancer progression. Oncol Rep. 2009; 21:1235–1241.
33. Nakajima M, Kato H, Miyazaki T, Fukuchi M, Masuda N, Fukai Y, Sohda M, Inose T, Sakai M, Sano A, Tanaka N, Ahmad F, Kuwano H. Prognostic significance of heat shock protein 110 expression and T lymphocyte infiltration in esophageal cancer. Hepatogastroenterology. 2011; 58: 1555–1560.
34. Gong W, Wang ZY, Chen GX, Liu YQ, Gu XY, Liu WW. Invasion potential of H22 hepatocarcinoma cells is increased by HMGB1-induced tumor NF-κB signaling via initiation of HSP70. Oncol Rep. 2013; 30:1249–1256.
35. Sims JD, McCready J, Jay DG. Extracellular heat shock protein (Hsp)70 and Hsp90α assist in matrix metalloproteinase-2 activation and breast cancer cell migration and invasion. PLoS One. 2011; 6:e18848.
36. Mandal AK, Gibney PA, Nillegoda NB, Theodoraki MA, Caplan AJ, Morano KA. Hsp110 chaperones control client fate determination in the hsp70-Hsp90 chaperone system. Mol Biol Cell. 2010; 21:1439–1448.
37. Hosaka S, Nakatsura T, Tsukamoto H, Hatayama T, Baba H, Nishimura Y. Synthetic small interfering RNA targeting heat shock protein 105 induces apoptosis of various cancer cells both *in vitro* and *in vivo*. Cancer Sci. 2006; 97:623–632.
38. Association JGC. Japanese classification of gastric carcinoma: 3rd English edition. Gastric Cancer. 2011; 14:101–112.

Yamauchi et al. Surgical Case Reports (2016) 2:15
DOI 10.1186/s40792-016-0142-9

Surgical Case Reports
a SpringerOpen Journal

CASE REPORT Open Access

Poorly cohesive adenocarcinoma of the ampulla of Vater: a case report

Hayato Yamauchi[1*], Shinji Sakurai[2], Kei Hagiwara[1], Tomonori Yoshida[1], Yuichi Tabe[1], Takaharu Fukasawa[1], Shinsuke Kiriyama[1], Minoru Fukuchi[1], Hiroshi Naitoh[1] and Hiroyuki Kuwano[3]

Abstract

A 47-year-old Japanese male was submitted to pancreaticoduodenectomy for an ampullary cancer. Pathologically, the ampullary cancer was poorly cohesive adenocarcinoma without tubular structure. Moreover, locoregional lymph nodes were swollen with hypervascularity, plasmacytes infiltration, and hemorrhage. Our case seems to be different from usual poorly differentiated adenocarcinoma.

Keywords: Ampullary cancer, Cohesive adenocarcinoma, Poorly differentiated adenocarcinoma

Background

Ampullary carcinoma is a malignant tumor arising in the last centimeter of the common bile duct, and patients with these tumors have been reported to have a relatively favorable prognosis after surgical resection [1]. Among the tumors originated from the ampulla of Vater, poorly differentiated adenocarcinoma is a very rare disease [2] and the clinical outcomes of the patients are undetermined. On the other hand, Castleman's disease (CD) is a lymphoproliferative disorder which was first described by Dr. Benjamin Castleman in 1956 and which often develops in the retroperitoneal lymph nodes [3].

Here, we present a rare case of poorly cohesive adenocarcinoma of the ampulla of Vater without tubular structure, the histology of which is similar to poorly cohesive adenocarcinoma of the stomach. The swollen locoregional lymph nodes showed marked plasma cells infiltration, vascular proliferation like CD and hemorrhage, but no lymph node metastasis of the tumor was found.

Case presentation

The patient was a 47-year-old man who had no pathological antecedents. He admitted to our hospital with hyperbilirubinemia of 1.6 mg/dl at health screening, with appetite loss and epigastralgia appearing 6 months ago. Carbohydrate antigen 19-9 and carcinoembryonic antigen were normal. Abdominal computed tomography and magnetic resonance imaging showed a dilatation of the common bile duct and a stone in the gallbladder. Neither tumor nor lymph nodes swelling were observed. No stones or abnormal arrangement of the pancreaticobiliary ductal union were found by an endoscopic retrograde cholangiopancreatography. Gastrointestinal endoscopy showed irregularly shaped concavity on the ampulla of Vater, and histology of the biopsy revealed signet ring cell carcinoma.

A pancreatoduodenectomy was performed. The final pathological diagnosis was poorly cohesive adenocarcinoma including signet ring cell carcinoma component in the Vater's ampulla without lymph node metastases (Fig. 1). The carcinoma consisted of complete poorly differentiated carcinoma cells most of which showed non-cohesive pattern, and tubular structure was not seen in any sections examined for pathological analysis (Fig. 2). Tumor invasion was seen around the common duct, bile duct, and pancreatic duct in the ampulla of Vater and the duodenum wall. A little lymphatic and vascular invasion was observed. Perineural invasion was little seen.

The locoregional lymph nodes were swollen with hemorrhage in the capsule. Lymph follicles were atrophic, and vascular hyperplasia was found in the germinal centers (Fig. 3). Marked plasma cell infiltration was seen in the interfollicular stroma (Fig. 4). However, hyalinization of the vascular wall was not seen. Histological findings resemble those of CD but are slightly different. Immunohistochemically, plasma cells in the interfollicular

* Correspondence: m07702048@gunma-u.ac.jp
[1]Department of Surgery, Japan Community Health Care Organization, Gunma Chuo Hospital, 1-7-13 Kouun-cho, Maebashi, Gunma 371-0025, Japan
Full list of author information is available at the end of the article

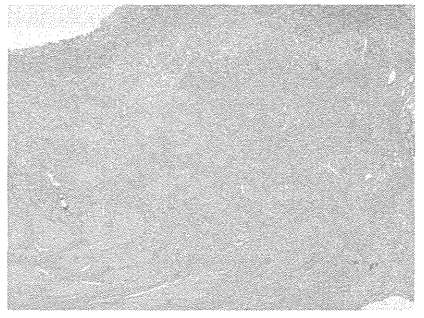

Fig. 1 Infiltrating carcinoma cells shows scirrhous appearance in the ampulla of Vater

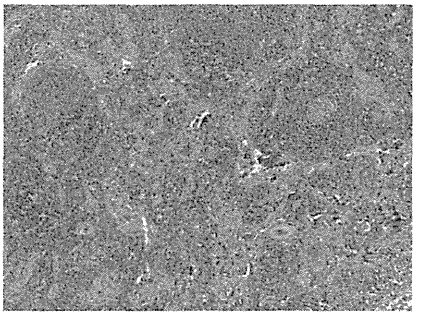

Fig. 3 Lymph follicles were atrophic, and vascular hyperplasia was found in the germinal centers

region were evenly positive for kappa and lambda light chain, which meant no evidence of clonal proliferation.

According to the TNM classification, the tumor was classified as pT3 N0 M0 ly1 v1 pn0 pstageIII. The patient remained well and had no evidence of locoregional and metastatic recurrence during the 28 months of follow-up.

Discussion

The primary adenocarcinoma of the ampulla of Vater is a rare tumor, and most ampullary adenocarcinomas are well differentiated [2]. Ampullary carcinomas are thought to arise from the glandular epithelium of the ampulla of Vater [4]. It has been suggested that molecular biologically ampullary carcinoma is different from bile duct and pancreatic carcinomas, whereas that share the same molecular biological characteristics with duodenal carcinomas [1]. The clinical outcome of ampullary carcinoma has been reported to be better than those of bile duct and pancreatic carcinomas [1]. Thus, it would be important to distinguish the origin of carcinomas developed around the region of the ampulla of Vater.

The present case was diagnosed as ampullary carcinoma, since the tumor invaded both the common bile duct and the biliary and pancreatic ducts in the duodenal wall. However, the tumor in our case was non-cohesive type of poorly differentiated adenocarcinoma, in which glandular structure was not observed in any of specimens, and the histology resembled scirrhous carcinoma of the stomach, which was classified into poorly cohesive carcinoma according to World Health Organization (WHO) classification. To our knowledge, this type of carcinoma is uncommon in any of the ampulla of Vater, pancreatic duct, and bile duct [2, 5]. Thus, poorly cohesive carcinoma was listed only in the stomach, but not in the bile duct, pancreas, and the ampullary region in WHO classification.

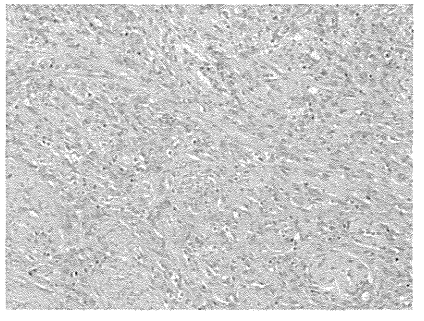

Fig. 2 The proliferating tumor cells consist of poorly cohesive adenocarcinoma without tubular structure

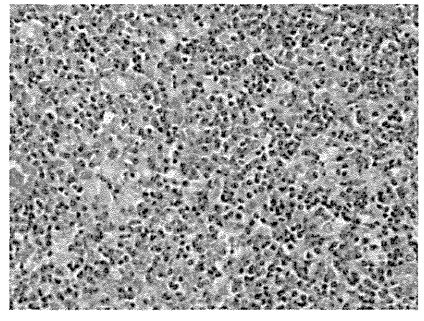

Fig. 4 Marked plasma cell infiltration was observed in the interfollicular stroma

On the other hand, tumors of ampulla of Vater are categorized into bile duct carcinoma in Japanese classification [6]. Most extrahepatic cholangiocarcinomas have been reported to be histologically well-to-moderately differentiated adenocarcinomas [7]. As far as we researched in the PubMed, there has been no report about exclusively poorly cohesive adenocarcinoma of periampullary region. Thus, our case which consists of pure poorly cohesive carcinoma cells without tubular structure is thought to be quite rare.

However, our case was classified into poorly differentiated type of tubular adenocarcinoma (tub3) according to the General Rules for Surgical and Pathological Studies on Cancer of the Biliary Tract, Japanese Society of Biliary Surgery [6], because Japanese classification also did not have poorly cohesive carcinoma in the bile duct carcinoma as same as WHO classification.

Our patient underwent curative pancreatoduodenectomy. The poorly differentiated adenocarcinoma has been reported to exhibit higher probability of recurrence and show poor prognosis compared with other histological types after the curative resection [8–11]. The prognostic factors of ampullary carcinoma after resection include lymph node metastasis, pancreatic invasion, and perineural invasion [12, 13]. These histological findings are also the most important prognostic factors for bile duct carcinoma after curative resection [14, 15]. However, our case showed a little vascular invasion and perineural invasion without nodal metastasis in spite of the case of poorly differentiated carcinoma, which might indicate better prognosis than usual poorly differentiated adenocarcinoma.

Histopathologically, the cause of lymph node swelling was not due to the tumor metastasis but the CD-like change and hemorrhage. CD is a rare atypical lymphoproliferative disorder. And soon after the original presentation of Castleman et al., CD has been subdivided into a hyaline vascular and plasma cell histopathological pattern, with intermediate variants [16]. The pathological findings of the locoregional lymph nodes in our case revealed hypervascular germinal centers with marked interfollicular plasma cell infiltration, which are common features of CD. However, hyalinization of the proliferating vessel was not observed, which was different from CD. The patient has no past history related to immune dysregulation. Therefore, we could not definitely diagnose the patient as CD.

Conclusions

We report a rare case of poorly cohesive adenocarcinoma in the ampulla of Vater with enlarged lymph nodes like CD. The relation between clinicopathological features and the long-term outcomes are not clear only in this case. The histopathological findings of our case seem to be different from those of poorly differentiated adenocarcinoma, and it would be better to add poorly cohesive adenocarcinoma to the histopathological classification of the ampulla of Vater and bile duct.

Consent

Written informed consent was obtained from the patient for publication of this case report and any accompanying images. A copy of the written consent is available for review by the Editor-in-Chief of this journal.

Abbreviations

CD: Castleman's disease; WHO: World Health Organization.

Competing interests

The authors declare that they have no competing interests.

Authors' contributions

HT and SS participated in the patient's care, research design, performance of the research, data analysis, and writing of the paper. KH, TY, YT, TF, SK, and MF participated in the patient's care and data collection. HN and HK participated in revising the manuscript critically. All authors read and approved the final manuscript.

Authors' information

HY, KH, TY, YT, TF, SK, MF, and HN are the staff surgeons at the Department of Surgery, Japan Community Health care Organization, Gunma Chuo Hospital. SS is a staff pathologist at the Department of Diagnostic Pathology, Japan Community Health care Organization, Gunma Chuo Hospital. HK is the professor at the Department of General Surgical Science (Surgery I), Gunma University, Graduate School of Medicine.

Author details

[1]Department of Surgery, Japan Community Health Care Organization, Gunma Chuo Hospital, 1-7-13 Kouun-cho, Maebashi, Gunma 371-0025, Japan. [2]Department of Diagnostic Pathology, Japan Community Health Care Organization, Gunma Chuo Hospital, Gunma, Japan. [3]Department of General Surgical Science (Surgery I), Gunma University, Graduate School of Medicine, Gunma, Japan.

Received: 18 August 2015 Accepted: 11 February 2016
Published online: 15 February 2016

References

1. Sarmiento JM, Nagorney DM, Sarr MG, Farnell MB. Periampullary cancers: are there differences? Surg Clin North Am. 2001;81(3):543–55.
2. Terada T. Pathologic observations of the duodenum in 615 consecutive duodenal specimens in a single Japanese hospital: II. Malignant lesions. Int J Clin Exp Pathol. 2012;5(1):52–7.
3. Castleman B, Iverson L, Menendez VP. Localized mediastinal lymphnode hyperplasia resembling thymoma. Cancer. 1956;9(4):822–30.
4. Buck JL, Elsayed AM. Ampullary tumors: radiologic-pathologic correlation. Radiographics. 1993;13(1):193–212.
5. Kanthan R, Gomez D, Senger JL, Kanthan SC. Endoscopic biopsies of duodenal polyp/mass lesions: a surgical pathology review. J Clin Pathol. 2010;63(10):921–5.
6. Japanese Society of Biliary Surgery. General rules for surgical and pathological studies on cancer of the biliary tract. 5th ed. Tokyo: Kanehara; 2011.
7. Nakanuma Y, Curado MP, Franceschi S, Gores G, Paradis V, Sripa B. Intrahepatic cholangiocarcinoma. In: Bosman FT, Carneiro F, Hruban RH, Theise ND, editors. World Classification of Tumours of the Digestive System. Lyon: IARC; 2010. p. 217–24.
8. Kohler I, Jacob D, Budzies J, Lehmann A, Weichert W, Schulz S. Phenotypic and genotypic characterization of carcinomas of the papilla of Vater has prognostic and putative therapeutic implications. Am J Clin Pathol. 2011;135(2):202–11.
9. Westgaard A, Tafjord S, Farstad IN, Cvancarova M, Eide TJ, Mathisen O. Pancreatobiliary versus intestinal histologic type of differentiation is an

independent prognostic factor in resected periampullary adenocarcinoma. BMC Cancer. 2008;8:170.
10. Carter JT, Grenert JP, Rubenstein L, Stewart L, Way LW. Tumors of the ampulla of vater: histopathologic classification and predictors of survival. J Am Coll Surg. 2008;207(2):210–8.
11. Park JS, Yoon DS, Kim KS, Choi JS, Lee WJ, Chi HS. Factors influencing recurrence after curative resection for ampulla of Vater carcinoma. J Surg Oncol. 2007;95(4):286–90.
12. Kondo S, Takada T, Miyazaki M, Miyakawa S, Tsukada K, Nagino M. Guidelines for the management of biliary tract and ampullary carcinomas: surgical treatment. J Hepatobiliary Pancreat Surg. 2008;15(1):41–54.
13. Gheza F, Cervi E, Pulcini G, Villanacci V, Giulini SM, Schiavo-Lena M. Signet ring cell carcinoma of the ampulla of Vater: demonstration of a pancreatobiliary origin. Pancreas. 2011;40(5):791–3.
14. He P, Shi JS, Chen WK, Wang ZR, Ren H, Li H. Multivariate statistical analysis of clinicopathologic factors influencing survival of patients with bile duct carcinoma. World J Gastroenterol. 2002;8(5):943–6.
15. He P, Shi J, Chen W, Wang Z. Multivariate analysis by Cox proportional hazards model on prognoses of patients with bile duct carcinoma after resection. Chin Med J (Engl). 2002;115(10):1538–41.
16. Palestro G, Turrini F, Pagano M, Chiusa L. Castleman's disease. Adv Clin Path. 1999;3(1–2):11–22.

Apoptosis-mediated antiproliferative activity of friedolanostane triterpenoid isolated from the leaves of *Garcinia celebica* against MCF-7 human breast cancer cell lines

ANAS SUBARNAS[1], AJENG DIANTINI[1], RIZKY ABDULAH[1,2], ADE ZUHROTUN[3], PATRIA A. NUGRAHA[1], YUNI E. HADISAPUTRI[4], IRMA M. PUSPITASARI[1,2], CHIHO YAMAZAKI[2], HIROYUKI KUWANO[4] and HIROSHI KOYAMA[2]

[1]Department of Pharmacology and Clinical Pharmacy, Faculty of Pharmacy, Universitas Padjadjaran, Jatinangor 45363, Indonesia; [2]Department of Public Health, Gunma University Graduate School of Medicine, Gunma 371-8511, Japan; [3]Department of Biological Pharmacy, Faculty of Pharmacy, Universitas Padjadjaran, Jatinangor 45363, Indonesia; [4]Department of General Surgical Science, Gunma University Graduate School of Medicine, Gunma 371-8511, Japan

Received July 31, 2015; Accepted October 2, 2015

DOI: 10.3892/br.2015.532

Abstract. The leaves of *Garcinia celebica* strongly inhibit the proliferation of MCF-7 human breast adenocarcinoma cell lines. The present study focused on investigating the active anticancer and antiproliferative compound from the *G. celebica* leaves and assessing its mechanism of action. Ethanol extracts of *G. celebica* were fractionated based on their polarity using *n*-hexane, ethyl acetate and water. The antiproliferative properties were tested *in vitro* against MCF-7 human breast cancer cell lines using the 3-(4,5-dimethylthiazolyl-2)-2,5-diphenyltetrazolium bromide assay. The active compound was subsequently isolated using column chromatography and identified by nuclear magnetic resonance. The characterized compound was also tested for its antiproliferative properties and the mechanism by which it induces apoptosis in MCF-7 cells by western blot analysis of the activated apoptotic proteins. This resulted in the isolation of a friedolanostane triterpenoid, which was determined to be methyl-3α, 23-dihydroxy-17,14-friedolanstan-8,14,24-trien-26-oat. This compound inhibited MCF-7 cell proliferation in a time- and dose-dependent manner with IC_{50} values of 82 and 70 μM for the 24 and 48 h treatments, respectively. Furthermore, the western blot analysis suggested that the compound exerted its anticancer activities by promoting apoptosis through the inhibition of the oncogenic protein Akt, thereby increasing the expression of poly (ADP-ribose) polymerase (PARP) protein. These results suggest that methyl-3α,23-dihydrox y-17,14-friedolanstan-8,14,24-trien-26-oat is the anticancer compound found in *G. celebica*, providing a basis for its potential use in cancer disease management.

Correspondence to: Professor Anas Subarnas, Department of Pharmacology and Clinical Pharmacy, Faculty of Pharmacy, Universitas Padjadjaran, Jl. Raya Bandung Sumedang KM 21, Jatinangor 45363, Indonesia
E-mail: aasubarnas@yahoo.co.id

Key words: Garcinia celebica, primates, cancer, apoptosis

Introduction

Cancer remains an extremely serious life-threatening disease for all humans. Although continuous efforts have been made to provide novel leads against cancers, and numerous cancer drugs have been derived from plants or generated synthetically, the current drugs used clinically have no significant effectiveness or safety (1). Therefore, it is important to undertake research into the discovery of new anticancer drugs of plant origins. Numerous types of bioactive compounds have been isolated from medicinal plants and several of these compounds are currently undergoing further investigation (2).

As plants consumed by primates are assumed to be a promising source of therapeutic agents for human disease management, a series of studies have been conducted to search for anticancer agents from plant sources with a focus on finding new potential drugs or leads for breast cancer from primate-consumed plants (3). Breast cancer is the most malignant form of cancer among women, causing >1.2 million new cases and 0.5 million mortalities annually (4). Our previous studies revealed that kaempferol-3-*O*-rhamnoside, isolated from the leaves of *Schima walichii* Korth, a plant commonly consumed by primates, inhibited the proliferation of the MCF-7 breast cancer cell line through activation of the caspase cascade pathway (5). Furthermore, an evaluation of 42 species of Indonesian primate-consumed plants revealed that several plant extracts, including the *n*-hexane fraction of the *Garcinia celebica* (*G. celebica*) leaves extract, had potent antiproliferative activity against MCF-7 cells (6). In the present study, a compound from the *n*-hexane fraction of the *G. celebica* leaves extract with antiproliferative activity against MCF-7 cell lines was identified and the pro-apoptotic activity of the active compound was evaluated.

Materials and methods

Collection of plant materials. Leaves of *G. celebica* were collected in the Pangandaran Beach Conservation Area of West Java (Indonesia). The plant species was identified by the Department of Biology, Faculty of Mathematics and Natural Sciences, Universitas Padjadjaran (Jatinangor, Indonesia). The leaves were dried in the open air away from direct sunlight.

Isolation of an active compound. Dried *G. celebica* leaves were powdered and extracted with 95% ethanol (three times every 24 h) at room temperature and the solvent was evaporated under reduced pressure at 50˚C to yield concentrated extracts. The extract was partitioned with a mixture of *n*-hexane-water (3:1) to generate hexane and water layers. The water layer was further extracted with ethyl acetate to yield ethyl acetate and water fractions. The *n*-hexane and ethyl acetate fractions had inhibitory activities against MCF-7 cell proliferation. Silica gel chromatography was used to elute the *n*-hexane fraction (23.32 g) into 5 fractions of *n*-hexane-ethyl acetate mixtures with increasing polarity (*n*-hexane:ethyl acetate, 9:1, 8:2, 7:3, 6:4, 5:5). Each fraction was tested for its toxicity against *A. salina* larvae (7), and the fraction with the highest toxicity was further chromatographed over silica gel with the same elution system to generate 11 fractions, of which fraction 6 contained the targeted compounds. Fraction 6 was subjected to preparative thin-layer chromatography using a mixture of chloroform-methanol (9.5:05) as a developing solvent system. The application of preparative chromatography resulted in a compound (50.20 mg, white amorphous solid) that showed high toxicity against *A. salina* larvae. The compound was identified by an analysis of its spectroscopic data [ultraviolet (UV), infrared (IR), mass spectrometry (MS) and nuclear magnetic resonance (NMR)].

Cell culture and drug-sensitivity assays. MCF-7 human breast cancer cell lines were purchased from the American Type Culture Collection (Manassas, VA, USA). The cell lines were cultured in RPMI-1640 medium (Sigma-Aldrich, St. Louis, MO, USA) supplemented with 10% fetal bovine serum and antibiotics (100 U/ml penicillin and 100 μg/ml streptomycin). Cell proliferation was analyzed using an 3-(4,5-dimethylthiazolyl-2)-2,5-diphenyltetrazolium bromide (MTT) assay in cells treated with various concentrations of the active compound isolated from leaves of *G. celebica* following the methods of Abdulah *et al* (8). Briefly, $2x10^4$ cells in 50 μl/well were plated in 96-well plates. Following the initial cell seeding, different concentrations of the active compound isolated from leaves of *G. celebica* were added and incubated for 24 h. WST-8 assay cell-counting solution (Dojindo Lab., Kumamoto, Japan) was added to each well (10 μl) and incubated at 37˚C for 3 h. After the addition of 100 μl/well of 1 N HCl, the cell proliferation rate was subsequently determined by measuring the absorbance at a wavelength of 450 nm. The absorbance was read using a microtiter plate reader (Becton-Dickinson, Franklin Lakes, NJ, USA).

Cell extraction and western blot analysis. Protein concentrations were determined using a bicinchoninic acid protein assay kit (Pierce Biotechnology, Inc., Rockford, IL, USA). In total, 40 μg protein was electrophoresed on a Mini-PROTEAN TGX Precast gel (4-20%; Bio-Rad Laboratories, Hercules, CA, USA) and electrotransferred to a 7x8 cm Hybond-enhanced chemiluminescence membrane (GE Healthcare Life Sciences, Little Chalfont, UK). Apoptosis-associated proteins were analyzed by immunoblot analysis using poly(adenosine diphosphate-ribose) polymerase (PARP; #9542) and Akt (#4685) antibodies at a 1:1,000 dilution (both Cell Signaling Technology, Danvers, MA, USA). β-actin (#A5441; Sigma-Aldrich) served as the loading control.

Results

Structural determination of methyl-3α,23-dihydroxy-17,14-friedolanstan-8,14,24-trien-26-oat from G. celebica leaves. An antiproliferative compound isolated from the leaves of *G. celebica* was amorphous and was white in color. It exhibited a molecular ion peak at *m/z* 484 in the electron ionization mass spectrum indicating that this compound had a molecular formula of $C_{31}H_{48}O_4$.

The UV spectrum indicated absorption bands at 275 and 439 nm and the IR spectrum revealed the presence of a hydroxyl group (3,500 cm^{-1}) and a carbonyl group of an α,β-unsaturated ester (1,700 cm^{-1}). The presence of the carbonyl functionality was further confirmed by a carbon signal appearing at δ 168.7 in the ^{13}C NMR spectrum.

The ^1H and ^{13}C NMR spectra of the compound exhibited that this compound was assumed to be a triterpenoid compound. The ^1H NMR spectrum indicated the presence of 5 tertiary methyls (δ 0.76, 0.89, 0.90, 0.98 and 1.01), 1 secondary methyl (δ 0.94, *d*, J=7.5 Hz), and 1 oxymethine proton (δ 3.45, *br s*). These signals were assumed due to a tetracyclic triterpene having a 3α-hydroxy group (9-11). Furthermore, signals due to 1 olefinic proton (δ 6.72, *qd*, J=7.5 and 1.5 Hz), 1 vinylic methyl (δ 1.87, *d*, J=1.5 Hz), 1 oxymethine proton (δ 4.57, *ddd*, J=10.7, 7.5 and 2.5 Hz), and methoxy protons (δ 3.75, *s*) were observed. These signals suggested that the compound had a side chain with a structure of [-$CH(Me)CH_2CH(OH)CH=C(Me)COOCH_3$]. The ^{13}C NMR spectrum indicated the presence of 7 methyl carbons (δ 12.9, 15.5, 15.8, 17.3, 19.2, 22.4 and 28.2), 8 methylene carbons (δ 18.3, 22.9, 25.8, 26.9, 29.4, 30.3, 39.7 and 45.7), 6 methine carbons (δ 33.6, 44.6, 67.1, 76.0, 116.0 and 142.6), and 9 quartenary carbons (δ 37.8, 38.0, 48.2, 50.2, 123.1, 127.3, 144.6, 148.9 and 168.7). These NMR spectral data showed that the compound may be friedolanostane triterpenoid with one tetrasubstituted double bond and two trisubstituted double bonds. One of the two trisubstituted double bonds was located in the side chain and the two remaining double bonds in the tetracyclic system were indicated to be conjugated. The conjugated double bonds were assumed to be present at C-8/C-9 and C-14/C-15, therefore, the vinylic proton appearing at 5.26 (*s*) was at C-15. Thus, the structure of the compound was established as methyl-3α, 23-dihydroxy-17,14-friedolanstan-8,14,24-trien-26-oat (Fig. 1) which has been reported previously. The ^1H and ^{13}C NMR data of the identified compound is shown in Table I. Confirmation of the structure was obtained by comparison of its spectral data with those reported in previous studies (11,12).

Inhibitory activity of methyl-3α,23-dihydroxy-17,14-friedolanstan-8,14,24-trien-26-oat against MCF-7 cell line